Site-specific glycan analysis of human chorionic gonadotropin β-subunit from malignancies and pregnancy by liquid chromatography – electrospray mass spectrometry

Leena Valmu[a]*, Henrik Alfthan[a], Kristina Hotakainen[a], Steven Birken[b] and Ulf-Håkan Stenman[a]

[a] Department of Clinical Medicine, Division of Clinical Chemistry, Biomedicum, University of Helsinki, PB 63 (Haartmaninkatu 8), FIN-00014, Finland.

[b] Department of Obestrics and Gynecology, Columbia University College of Physicians & Surgeons, New York, NY 10032

Running title: Characterization on hCGβ glycans

Keywords: Cancer/ hCG/Mass spectrometry/N-glycosylation/O-glycosylation / hyperglycosylated hCG/antibody B152

*Address for correspondence:

Dr. Leena Valmu

Department of Clinical Medicine

Division of Clinical Chemistry

Biomedicum Helsinki

P.O.Box 63 (Haartmaninkatu 8)

FIN-00014 University of Helsinki,

Finland

Tel: +358-9-47171735

Fax: +358-9-47171731

Email: leena.valmu@helsinki.fi

Abstract

Glycosylation is an important post-translational modification in proteins and aberrant glycosylation occurs in malignancies. Human Chorionic Gonadotropin (hCG) is a glycoprotein hormone produced in high concentrations during pregnancy. It is also expressed as particular glycoforms by certain malignancies. These glycoforms, which are called "hyperglycosylated" hCG, have been reported to contain more complex glycan moieties. We have analyzed tryptic glycopeptides of the β-subunit of hCG of various origins by liquid chromatography connected to an electrospray mass spectrometer. Site-specific glycan structures were visualized by use of differential expression analysis software.

HCGβ was purified from urine of two patients with testicular cancer, one with choriocarcinoma, one with an invasive mole, two pregnant women at early and late gestation, from a pharmaceutical preparation and culture medium of a choriocarcinoma cell line. N-glycans at Asn-13 and Asn-30 as well as O-glycans at Ser-121, Ser-127, Ser-132 and Ser-138 were characterized.

In all samples the major type of N-glycan was a biantennary complex-type structure, but triantennary structures linked to Asn-30 as well as fucosylation of the Asn-13 bound glycan are increased in cancer-derived hCGβ. There were significant site-specific differences in the O-glycans with constant core-2 glycans at Ser-121, core-1 glycans at Ser-138 and putative sites unoccupied by any glycan. Core-2 glycans at either Ser-127 or Ser-132 were enriched in cancer. The glycans of free hCGβ were larger and had a higher fucose content of Asn-13 linked oligosaccharides than intact hCG. This may facilitate detection of this malignancy- associated variant by a lectin assay. Analysis of hyperglycosylated hCG affinity-purified with antibody B152 confirmed that this antibody recognizes a core-2 glycan on Ser-132.

Introduction

Glycosylation is one of the most important and common post-translational protein modifications. It may affect both protein structure and function but the impact of glycosylation is protein dependent. Because changes in protein glycosylation are associated with numerous diseases, including cancer (Hakomori, S. 2002), protein glycosylation is important in clinical research.

Recent advances in glycoproteomics, a field combining proteomics and glycomics, have been greatly influenced by methodological development. Especially mass spectrometry (MS) provides important structural information on glycoproteins (Harvey, D.J. 2001). MS analysis of glycoproteins based on release of glycans either enzymatically or chemically provides structural glycan information but the information on site occupancy is lost. Analysis of glycopeptides obtained by proteolytic digestion, typically with trypsin, provides site-specific glycan information, but this approach may be hampered by difficulties in digestion of resistant glycoproteins. Furthermore, the analysis is often complicated by the heterogeneity of structurally related oligosaccharides occupying a single glycosylation site.

Human chorionic gonadotropin (hCG) is a glycoprotein hormone produced by placental trophoblasts and trophoblastic tumors. HCG is a heterodimer composed of α and β subunits (hCGβ). The α subunit is shared with the other glycoprotein hormones, luteinizing hormone, follicle stimulating hormone and thyroid stimulating hormone, whereas the β subunit is specific for each hormone. HCG is expressed throughout gestation and it occurs at high concentrations both in serum and urine of pregnant women.

About one third of the molecular weight of hCG consists of carbohydrates and glycosylation is of structural and functional importance affecting both the half-life in circulation and the signal transduction induced by this hormone (Lustbader, J.W., Lobel, L., et al. 1998). The glycosylation pattern of hCG has been extensively studied. Two asparagine-linked carbohydrate units (N-glycans) on hCGβ at Asn-13 and Asn-30 (Carlsen, R.B., Bahl, O.P., et al. 1973) have been shown to consist of biantennary, complex-type N-glycans with terminal sialic acids and a variable content of fucose (Kessler, M.J., Reddy, M.S., et al. 1979, Weisshaar, G., Hiyama, J., et al. 1991). The site-specific N-glycan structures have been further characterized by mass spectrometry using matrix-assisted laser desorption ionization (MALDI) technique (Jacoby, E.S., Kicman, A.T., et al. 2000, Laidler, P., Cowan, D.A., et al. 1995) and liquid chromatography (LC) – electrospray ionization (ESI) MS (Liu, C. and Bowers, L.D. 1997). Four serine-linked oligosaccharides (O-glycans) attached to serine residues 121, 127, 132 and 138 have been shown to consist of monoantennary, so-called core-1 O-glycan structures with two sialic acids attached to each glycan (Kessler, M.J., Mise, T., et al. 1979). However, core-2 type O-glycan at Ser-121 as well as putative glycosylation sites apparently not glycosylated have also been detected (Liu, C. and Bowers, L.D. 1997). All MS studies on the glycan structure of hCG have been performed using pharmaceutical hCG preparations that have been partially purified from pooled urine from pregnant women.

Except in pregnancy, hCG is expressed by certain malignancies and especially by trophoblastic and testicular germ cell tumors, for which hCG is a sensitive marker (Stenman, U.H., Alfthan, H., et al. 2004). Furthermore, the concentration of free hCGβ in serum is often elevated in patients with nontrophoblastic cancers and this is a sign of adverse prognosis (Alfthan, H., Haglund, C., et al. 1992, Stenman, U.H.,

Alfthan, H., et al. 2004). Various isoforms of hCG have been shown to be associated with malignancies. These include "nicked" hCG (hCGn), in which several peptide bonds in loop 2 of hCGβ are cleaved (Birken, S., Krichevsky, A., et al. 1999, Puisieux, A., Bellet, D., et al. 1990) as well as "hyperglycosylated" hCG (hCGh), which is the major form of hCG in trophoblastic cancer (Birken, S., Krichevsky, A., et al. 1999, Elliott, M.M., Kardana, A., et al. 1997) and early pregnancy (Kovalevskaya, G., Birken, S., et al. 2002). hCGh has also been associated with Down's syndrome (Cole, L.A., Shahabi, S., et al. 1999) and early pregnancy loss (Kovalevskaya, G., Birken, S., et al. 2002). Tumor-derived hCGh has been shown to contain increased amounts of triantennary N-glycans (Elliott, M.M., Kardana, A., et al. 1997), abnormal biantennary N-glycans (Kobata, A. and Takeuchi, M. 1999), and biantennary core-2 type O-glycans (Birken, S., Yershova, O., et al. 2003, Elliott, M.M., Kardana, A., et al. 1997).

Most studies on the carbohydrates of hCGh have been performed by chromatographic analysis of glycans released from the polypeptide and this gives no site-specific structure information (Elliott, M.M., Kardana, A., et al. 1997, Mizuochi, T., Nishimura, R., et al. 1983). An antibody to hCG, B152 (Birken, S., Krichevsky, A., et al. 1999), recognizes a core-2 type O-glycan attached to Ser-132 and surrounding peptide structures in hCGβ (Kovalevskaya, G., Birken, S., et al. 2002) (Birken, S., Yershova, O., et al. 2003). All clinical studies on hCGh have been based on the use of this antibody. No studies on site-specific oligosaccharide heterogeneity of cancer-derived forms of hCG, which are often lumped together under the term "hyperglycosylated" (Birken 2003), have been performed.

In this study we have used novel differential expression analysis software to analyze site specific glycan structures of hCGβ from various sources by LC-MS of tryptic protein fragments.

Results

Characterization of hCGβ purified from urine

HCG was purified from urine by serial immunoaffinity chromatography and gel filtration. Purified hCG was reduced and alkylated with 4-vinyl pyridine causing dissociation of α and β subunits. HCGβ was isolated by reverse phase (RP) chromatography and its purity was checked by SDS-PAGE and further by LC-MS analysis of tryptic peptides. All the potential tryptic peptides without attached glycans were visualized by LC-MS analysis with better than 20 ppm mass accuracy (**Table I**). The identity of the peptides was verified by LC-MSMS identification (data not shown). In addition to the predicted tryptic cleavage sites, additional cleavage sites were observed in peptides 5 and 9 (data not shown). The cleavage pattern of peptide 5 is in agreement with the proposed cleavage of loop 2 in the β-subunit in nicked hCG (hCGn) (Cole, L.A., Kardana, A., et al. 1991), but in contrast to a previous report (Elliott, M.M., Kardana, A., et al. 1997) the major sites cleaved were after amino acids 45 and 49 with some minor cleavage after amino acids 44, 46 and 48. In P9 the major cleavage occurred after Asn-77, but minor cleavage was also seen after amino acids 76, 78, 79 and 80.

Of the putative N-glycan-containing peptides P3 and P4 as well as the O-glycan-containing peptides P13, P14 and P15, some lacking the glycan were also observed (**Table II**) but with minor intensities.

When the N-glycans of hCGβ were enzymatically removed by peptide-N-glycosidase F (PNGase F) a mass shift from 37 kDa to 29 kDa was observed by SDS-PAGE (data not shown). In LC-MS analyses of the tryptic digest, peptides P3 and P4

were detected at high intensity with a mass adduction of 1 Da due to conversion of asparagine to aspartic acids during PNGase F treatment (data not shown).

Site-pecific N-glycan analysis of hCGβ

For glycan analysis 3 pmol of hCGβ tryptic digest was subjected to capillary LC on a Atlantis dC18 column specially designed to retain hydrophilic peptides such as glycosylated ones. The LC-MS data generated was incorporated into DeCyder MS software, where 2D intensity maps were visualized (**Figure 1A**), with each spot representing the intensity of a peptide in a certain charge state separated based on its m/z value and retention time, *i.e.* hydrophilicity. The same peptide is represented by several charge states within the map. To identify tryptic peptides containing N-glycans, the 2D LC-MS patterns were compared using the DeCyder MS software PepMatch module to patterns of tryptic digests of hCGβ, from which the N-glycans had been enzymatically removed (**Figure 1B**). Two highly heterogeneous peptide patterns or "clouds" were observed for the N-glycosylated hCGβ peptides. In peptide-by-peptide analysis, peptides occurring at equal concentrations in the two digests (**Figure 1C**) were easily separated from peptides present only in the N-glycosylated molecule (**Figure 1D**). The identity of the differentially expressed peptides was studied by LC-MSMS fragmentation analysis (**Figure 1E**), which revealed sugar-specific oxonium ions (m/z 204 for HexNAc, 274 for NeuAc-H_2O, 292 for NeuAc, 366 for Hex-HexNAc, 657; NeuAc-Hex-HexNAc) as a result of oligosaccharide dissociation. In addition, a clear fragmentation profile of the attached oligosaccharide portion of the glycopeptide was seen. Minor peptide -derived y-ions could also be detected in some peptide fragmentations facilitating differentiation between the P3

and P4 containing glycans (**Figure 1A**). The deglycosylation of the Asn-30 attached oligosaccharides from P4 was incomplete in part of the peptides.

In the LC-MS analysis glycopeptides containing Asn-13-linked oligosaccharides were mainly preset as $[M+3H]^{3+}$ and $[M+4H]^{4+}$ with minor intensities of smaller peptides as $[M+2H]^{2+}$. Ion counts of all different charge states of the same peptide were summarized to calculate the intensity of each glycopeptide. The masses of the oligosaccharides attached to P3 were calculated by subtracting the theoretical polypeptide portion mass of 1418.8 Da from the observed deconvulated masses of glycosylated peptides. The sugar structures were thus derived by the mass matching approach (**Figure 2**). The same approach was used to calculate the oligosaccharides attached to Asn-30 in P4. Due to their larger mass, P4 glycopeptides appeared in the LC-MS analysis mainly as $[M+4H]^{4+}$ and $[M+5H]^{5+}$ with minor intensities as $[M+3H]^{3+}$. Analysis of the Asn-30 -attached oligosaccharides was complicated because Met-41 in P4 occurred both in native and oxidized form and the intensities of these needed to be summed together (**Figure 3**). Interestingly, incomplete deglycosylation of P4 with PNGase F was observed in P4 with oxidized Met-41 (**Figure 1B**).

The N-linked oligosaccharides attached to Asn-13 and Asn-30 in hCGβ purified from the urine of a pregnant woman at 35 weeks of pregnancy, from the urine of a patient suffering from invasive mole and from the urine of a patient with testicular cancer are shown in **Figures 2 and 3**. The relative intensities, which roughly represent the relative abundance of different glycan structures present, are shown with a value of 100 for the most intense component. Intensities of smaller glycan structures might be slightly increased relative to sialylated structures due to possible sialic acid release in mass spectrometric analysis. To simplify the picture of

the enormous oligosaccharide heterogeneity, glycan structures with a relative intensity less than 15 in all three samples are omitted from the figures, but they were taken into account for calculation of the proportion of all oligosaccharide structures shown in **Tables II and III**. In addition to the structures shown, some tetra-antennary glycans and some Asn-30 –linked oligosaccharides lacking fucose were observed.

Site-specific O-glycan analysis of hCGβ

The O-glycosylated tryptic peptides were difficult to detect by LC-MS analysis of the crude tryptic digest probably due to suppression by the enormous heterogeneity of N-glycan containing peptides. The C-terminal portion of hCGβ was therefore isolated by RP-HPLC after cleavage with GluC protease. The N-terminus of the fragment was confirmed to be the expected Ser-66 by LC-MSMS analysis of the fragment tryptic digest (data not shown).

Direct ESI-MS analysis of the purified C-terminal fragment showed a wide variety of heterogeneous masses. The deconvulated masses of the C-terminal hCGβ fragment from normal late pregnancy, invasive mole and testicular cancer are shown in **Figure 4**. Based on the masses observed, it was evident that sialylated core-2 structures were present at all four O-glycosylation sites in hCGβ purified from a testicular cancer patient (**Figure 4D**), whereas both core-1 and core-2 -containing structures were observed in molar disease and pregnancy. The small masses of the C-terminal peptide in pregnancy hCG (**Figure 4A**) showed that variants with some unoccupied O-glycosylation sites also existed.

The site specific O-glycan structures were studied in glycopeptides produced by tryptic digestion of the C-terminal fragment. Peptides P13 and P15, which contained Ser-121 and Ser-138 linked oligosaccharides, respectively, were almost

exclusively present as $[M+2H]^{2+}$. The major oligosaccharide structures assigned by the mass matching approach are shown in **Figure 5**. Ser-121 was constantly occupied by a core-2 glycan, whereas the core-1 structure always dominated at Ser-138 with some core-2 structure observed in malignancy. Both sites were also observed unoccupied by any glycan. Possibility that the exposure of small Tn and T antigens within these sites could be due to the desialylation in the mass spectrometric analysis can not be ruled out.

Analysis of P14 was complicated due to the presence of glycans on both Ser-127 and Ser-132 within the peptide. **Figure 5C** shows the observed masses, the major possible glycans and combinations of these in four groups: 1) one core-1, 2) two core-1 or one core-2, 3) one core-2 and one core-1 or 4) two core-2 O-glycans. A single oligosaccharide was detected in most of the P14 from pregnancy and invasive mole, thus, either Ser-127 or Ser-132 was not glycosylated in almost half of the hCGβ molecules. Either two core-1 glycans or one core-2 glycan made up most of the rest. These two had exactly the same mass and could not be differentiated by the mass matching approach. The largest mass of this group (2417.0) consists of either two intact core-1 structures with one sialic acid or one sialylated core-2 structure. The intense masses of 2126.0 and 1963.9 lacked either one sialic acid or in addition one hexose, respectively. In larger glycopeptides, visible mainly in P14 from testicular cancer, both glycosylation sites were occupied, but since different core-1 and core-2 structures could result in the same glycopeptide mass, the interpretation was difficult. However, the major structure (3073.3) contained a sialylated core-2 structure in one and an intact core-1 structure with one sialic acid in the other site. The glycopeptide with a mass of 3729.5 contained two sialylated core-2 oligosaccharides.

Differential glycan analysis of hCGβ in malignancy and pregnancy

Characteristic site-specific differences and similarities in the glycan structures were observed between hCGβ from patients with testicular cancer, choriocarcinoma, invasive mole, pregnant women of different gestational age and a pharmaceutical hCG preparation and hCG from JEG-3 cells (**Table II**). The oligosaccharide structures linked to Asn-13 showed no significant increase of triantennary structures in malignancy, whereas both triantennary and monoantennary oligosaccharides attached to Asn-30 were enriched in hCG from cancer patients. The degree of fucosylation in the two N-glycosylation sites varied. The Asn-30 linked oligosaccharides were mainly fucosylated, while fucosylation of Asn-13 linked glycans varied (**Table IIB**). Less than 25% of the oligosaccharides were fucosylated in hCGβ from late pregnancy and JEG cells, whereas the fucosylation degree exceeded 36% in hCGβ from malignancies.

Ser-121 in P13 contained a core-2 O-glycan structure irrespective of the source of hCG. In contrast, core-1 oligosaccharide structures containing either one or two sialic acids dominated at Ser-138. Especially in hCGβ from testicular cancer, but also to some extent in early pregnancy and JEG-3 cells, the core-2 structure was observed (**Figure 5, TableIIA**).

The two O-glycosylation sites of P14 displayed the largest variation between different hCGβ preparations. In pregnancy and molar disease, a single core-1 structure was most common with either one core-2 structure or two core-1 structures as the second most common form. In cancer patients and early pregnancy core-2 oligosaccharide structures were most often present in either one or in both sites. The glycan composition of the commercial hCG preparation resembled that in early pregnancy urine.

Fairly large individual differences were observed between the two samples from late pregnancy and the two testicular cancer patients. Thus, the patterns observed in this study are likely to represent only part of the true diversity.

Glycan analysis of hCGβ variants isolated from a single patient

Various forms of hCG were isolated from the patient with an invasive mole for site-specific glycan analysis. HCG was purified both from urine and serum and the hCGβ subunit was dissociated from the heterodimer. Very similar oligosaccharide structures and the same polypeptide chain cleavages in P5 and P9 occurred in hCG from serum and urine. In urinary hCGh isolated with MAb B152, core-2 O-glycans dominated in P14 and only 1% contained a single core-1 glycan. Interestingly, no N-glycan structure was enriched. Free hCGβ isolated from urine of this patient contained more triantennary N-glycans in P3 and P4 and more core-2 O-glycans in P14 than that in hCG and a higher proportion of the Asn-13 glycan was fucosylated (**Table III**).

Discussion

The present study confirms results of earlier ones (Elliott, M.M., Kardana, A., et al. 1997, Kobata, A. and Takeuchi, M. 1999) showing differences in the carbohydrate structure of hCGβ derived from pregnancy and malignant tumors, respectively. Furthermore, we demonstrate large differences in glycan structures between the different glycosylation sites and in hCG from various sources, which have not been characterized before.

We used an ESI-MS connected to a LC to analyze site-specific glycan structures in tryptic peptides of hCGβ. We, furthermore, used novel differential expression analysis software, designed for proteomics (Skold, K., Svensson, M., et al. 2002), to study differential abundance of oligosaccharide structures in the protein. Glycopeptides were identified by comparing the tryptic digest of a protein to a digest of the same deglycosylated molecule. Digests of the same protein purified from different sources and different isoforms of the same protein could also be compared. The combination of LC-MS analysis with differential expression analysis is especially useful for glycoproteins that, like hCG, are relatively easily digestible with proteases despite the oligosaccharides attached. This approach relies entirely on mass matching and it does not provide exact linkage information about the glycans. However, the glycan structures of hCG have been fairly extensively studied by enzymatic deglycosylation combined with mass spectrometric analysis and on the basis of this information it was possible to deduce structures solely by mass matching.

The N-glycosylation of hCG has been reported to be different in choriocarcinoma than in pregnancy (Elliott, M.M., Kardana, A., et al. 1997, Mizuochi, T., Nishimura, R., et al. 1983), but site-specific glycan differences of hCG

have not been studied. In present study, the earlier observed increase in the content of triantennary complex-type N-glycans in choriocarcinoma hCG (Elliott, M.M., Kardana, A., et al. 1997) was seen only in the oligosaccharides attached to Asn-30 but not in that attached to Asn-13. The earlier described increase in monoantennary N-glycans (Elliott, M.M., Kardana, A., et al. 1997) was observed in sugar structures attached to both Asn-13 and Asn-30. The abnormal biantennary N-glycan structures bearing both antennae within the same mannose residue detected in choriocarcinoma by Kobata et al (Kobata, A. and Takeuchi, M. 1999, Mizuochi, T., Nishimura, R., et al. 1983) could not be detected by the mass matching approach since these structures carry the same mass as ordinary biantennary N-glycans. Another site specific difference between the two N-glycans was the degree of fucosylation. Asn-30 linked glycans were nearly totally fucosylated, as earlier reported for pregnancy hCG (Kessler, M.J., Reddy, M.S., et al. 1979, Weisshaar, G., Hiyama, J., et al. 1991), whereas the fucosylation degree of Asn-13 linked oligosaccharides varied between 2 and 56%. Furthermore, fucosylation on Asn-13 attached glycans was enriched in malignancies and it was also higher in early than in late pregnancy. An increased fucose content of N-glycans in choriocarcinoma hCG with no site-specificity has earlier been reported in one study (Mizuochi, T., Nishimura, R., et al. 1983), but not in another one (Elliott, M.M., Kardana, A., et al. 1997).

Increased N-glycan fucosylation has previously been reported to occur in α-fetoprotein produced by hepatocellular carcinoma and this is of diagnostic value (Aoyagi, Y., Isemura, M., et al. 1985). Fucose on the first GlcNAc residue of complex-type N-glycans can be specifically recognized by *lens culinaris* agglutinin lectin. Lectins have also used to distinguish glycosylation differences in hCG from

pregnancy and choriocarcinoma cell lines, but LCA was not among the lectins studied (Kelly, L.S., Kozak, M., et al. 2005).

Reports on the O-glycosylation of hCGβ are controversial (Birken, S., Yershova, O., et al. 2003, Gervais, A., Hammel, Y.A., et al. 2003, Kessler, M.J., Mise, T., et al. 1979, Liu, C. and Bowers, L.D. 1997) and may be explained by the site-specific O-glycan difference observed in the present study. The core-1 structure has been found to dominate in pregnancy hCG, but we found that Ser-121 always contained a biantennary core-2 structure. This was previously suggested (Liu, C. and Bowers, L.D. 1997) but was not found in the original reports (Kessler, M.J., Mise, T., et al. 1979). The structure of this glycan was virtually identical in all the conditions studied. The oligosaccharide attached to Ser-138 was, on the other hand, in all samples studied mainly of core-1 type, with either one or two sialic acids attached. Core-2 structures were observed only in hCGβ purified from one testicular cancer patient, the choriocarcinoma cell line and very early pregnancy.

The occurrence of two O-glycosylation sites in P14, which is not specifically cleavable by known proteases, complicated the analysis of the oligosaccharide structures in Ser-127 and Ser-132. In spite of this, it was evident that in pregnancy only a single glycosylation site was occupied in a significant proportion of hCG, as earlier suggested (Liu, C. and Bowers, L.D. 1997). In most malignancy-derived hCG two glycosylation sites were occupied and two core-2 oligosaccharides were often detected. This is in agreement with the observation that MAb B152 recognizes a Ser-132 linked core-2 structure (Birken, S., Yershova, O., et al. 2003). The O-glycosylation of hCG purified from urine of a patient with an invasive mole resembled pregnancy-derived hCG while the N-glycosylation pattern was more similar to that in cancer-derived hCG. In very early pregnancy, the glycosylation of

P14 resembled that in cancer in that both sites were occupied. Some unique O-glycan structures have been observed in recombinant hCG (Gervais, A., Hammel, Y.A., et al. 2003) including O-glycan fucosylation and increased content of N-acetylhexosamine. These structures were not observed in the human hCG preparations analyzed in the present study. Thus they appear to represent oligosaccharides specific for the Chinese hamster ovary cell line used to express recombinant hCG.

In addition to glycans observed in the study, it is interesting to note that some glycosylation sites, notably Ser-138, Ser-121 and Asn-13, are not glycosylated in some of the hCG variants studied.

Most studies on hCG glycosylation have been performed on hCG prepared from pooled pregnancy urine (Kessler, M.J., Mise, T., et al. 1979, Kessler, M.J., Reddy, M.S., et al. 1979, Laidler, P., Cowan, D.A., et al. 1995, Liu, C. and Bowers, L.D. 1997, Weisshaar, G., Hiyama, J., et al. 1991) and thus the glycan structures observed can be expected to represent the average oligosaccharide composition of pregnancy hCG. In the commercial hCG preparation used in the present study a fairly high proportion of core-2 associated P14 was observed indicating that the preparation was mainly derived from first trimester urine. The choriocarcinoma cell line JEG-3 is a potential source of an hCGh standard for assays based on MAb B152. The N-glycan structures of JEG-3 derived hCG resembled that from early pregnancy including the degree of fucosylation and the content of triantennary glycan structures. The proportion of core-2 structures in P14 and P15 was as high as in hCG from cancer patients. This explains the strong reactivity of malignancy related hCG with MAb B152.

Various isoforms of hCG, including free hCGβ and hCGh, have been shown to be associated with malignancies (Alfthan, H., Haglund, C., et al. 1992, Elliott,

M.M., Kardana, A., et al. 1997). We, therefore, isolated free hCGβ and hCGh from urine and purified hCG from serum and urine of a patient with an invasive mole. Interestingly, the oligosaccharides of hCG isolated from serum displayed exactly the same glycan pattern as hCG purified from urine. Therefore, the heterogeneous oligosaccharide structures of urinary hCG are not modified by additional degradation in urine. In hCGh isolated with MAb B152, an increase in core-2 containing P14 was seen, but no other difference in glycan composition, except a small increase in triantennary Asn-30 associated glycan, was observed. The degree of fucosylation in the Asn-13 linked glycan was not changed. Therefore, the hCGh detected by MAb B152 differs markedly from "normal" hCG only with respect to the Ser-132 associated glycan. This confirms the finding that B152 recognizes this core-2 O-glycan and surrounding polypeptide structures (Birken, S., Yershova, O., et al. 2003).

Interestingly, the oligosaccharide structures of free hCGβ resembled that of "hyperglycosylated" hCG with a high proportion of triantennary N-linked glycans and core-2 type O-glycans. In addition, the fucosylation of the Asn-13 linked glycan was markedly elevated. This observation could indicate that the large glycans might inhibit the association of hCGβ with the α-subunit. The observation of malignancy-related "hyperglycosylation" of free hCGβ is in agreement with the fact that the proportion of hCGβ is increased in patients with throphoblastic cancer (Alfthan, H., Haglund, C., et al. 1992). Because fucosylated N-glycans react with *lens culinaris* agglutinin lectin, the malignancy associated hCGβ could possibly be detected with a lectin assay.

In conclusion, we characterized six site-specific glycan structures of hCG by differential expression analysis of LC-MS data on hCG isolated from pregnant women and patients with malignant diseases. Major differences were observed in the

fucosylation degree of Asn-13 linked glycans as well as the occurrence of core-2 O-glycans in Ser-127, Ser-132 and Ser-138. Furthermore, larger glycan structures and a higher degree of fucosylation of Asn-13 linked glycans was observed in free hCGβ than in heterodimeric hCG from the same patient. Analysis of hCGh isolated by affinity chromatography with MAb B152 confirmed that this antibody recognizes a core-2 glycan on Ser-132 and surrounding peptide structures.

Materials & Methods

Patients and samples

hCG was isolated from the urine of two patients with non-seminomatous testicular cancer (stages 1 and 3, respectively) (Sobin, L. and Wittekind, C. 2002), from one with choriocarcinoma (stage IIIA) and one with an invasive mole (stage IB) (Benedet, J. and Pecorell, S. 2000). Urine from one pregnant woman was collected at 5 and 7 weeks and from two women at 35 weeks after fertilization. Informed consent was obtained from all patients and the study was approved by the institutional ethics committee.

NaN_3 was added to a concentration of 0.5 g/L into the urine samples, which were stored at +4°C. hCG in the samples was quantitated by a time-resolved immunofluorometric assay performed as described (Alfthan, H., Haglund, C., et al. 1992, Pettersson, K., Siitari, H., et al. 1983).

The choriocarcinoma cell line, JEG-3 (American Type Culture Collections, ATCC) was cultured according to the guidelines provided. The hCG containing medium was centrifuged to remove cells and stored at -20°C. Pregnyl was purchased from Organon Technica and lot 167823 was used for analysis.

Purification of hCG

HCG was purified from 100-1000 mL of urine, containing 3-250 nmol/L of hCG. Urine was clarified by filtering through Nalgene disposable filter unit with 0.45 μm pore size and the filtrate was applied to an anti-hCG affinity column (1 ml) with a flow rate of 200 μL/min. MAb 6G5, raised in the laboratory as earlier described (Alfthan, H., Haglund, C., et al. 1992), was coupled CNBr activated Sepharose 4B

(Pharmacia) according to the instructions of the manufacturer. Prior to immunoaffinity chromatography the samples were passed through a precolumn of equal size with an unrelated MAb. The columns were equilibrated with 50 mmol/L sodium phosphate pH 7.4. After sample application the column was washed with 40 ml of 10 mmol/L ammonium acetate pH 4.5 and the bound protein eluted with 15 ml of 3 mol/L acetic acid. Fractions of 1 mL were collected and immediately neutralized with NH_4OH. Fractions containing hCG were pooled, concentrated using a Centricon centrifugal device with a cut-off of 10 kDa (Millipore) and fractionated by gel filtration on a Sephacryl S-100 HR (Amersham Biosciences) 16 x 700 mm column in 0.1 mol/L ammonium bicarbonate pH 8 with a flow rate of 200 µL/min. The content of intact hCG dimer and hCGβ in 800 µL fractions were determined by time-resolved immunofluorometric assays and the fractions containing hCG were freeze dried and stored at -20°C.

To separate free hCGβ from hCG, the urine was first applied to an affinity column containing MAb 9C11, raised in the laboratory and shown to be specific for free hCGβ (Alfthan, H., Haglund, C., et al. 1992). Bound hCGβ was eluted and further treated as described above. The flowthrough fraction was further applied to the anti-hCG affinity column containing MAb 6G5. HCGh was purified from urine by immunoaffinity chromatography with MAb B152 (Birken, S., Krichevsky, A., et al. 1999) column.

HCG was purified from a 5 mL serum sample from a patient with invasive mole containing 1800 nmol/L of hCG. The sample was first purified by gel filtration on a 16 x 700 mm column packed with Sephacryl S-200 HR (Amersham Biosciences) in 0.1 mol/L ammonium bicarbonate pH 8 at flow rate of 250 µL/min. Fractions containing proteins smaller than 70 kDa were collected and subjected to

immunoaffinity purification as described above. HCG was purified from the growth medium of JEG-3 cell line using MAb 6G5.

In-liquid alkylation and digestion of hCGβ

Purified hCG was reduced with dithiotreitol and alkylated with 4-vinylpyridine (Aldrich) in 6 mol/L guanidine hydrochloride, 2 mmol/L EDTA, 0.5 M Tris pH 7.5. The alkylated hCG with dissociated α and β subunits was desalted by RP-HPLC on a C4 column (Symmetry C4, 3.9 x 20 mm, 300 Å, 5 µm, Waters) and eluted with a linear gradient of acetonitrile (0-80 % in 30 min) in 0.1% TFA. HCGβ -containing fractions were pooled, dried and subjected to trypsin digestion using 10 % w/w sequencing grade trypsin (Promega Ltd) in 10 mmol/L ammonium bicarbonate at 37 °C for 16 h.

For digestion with Glu-C (V8, Roche), 5 % w/w protease was added in 50 mmol/L ammonium acetate pH 4 and digestion was carried out for 4 h at RT. After each incubation hour 2 % w/w V8 was added. The C-terminal portion of hCG was separated by RP chromatography on a C4 column (SymmetryC4, 2 x 50 mm, 300 Å, 3.5 µm, Waters). Proteolytic peptides were eluted with a linear gradient of acetonitrile (0-80 % in 30 min) in 0.1% TFA with a flow rate of 0.2 mL/min. Fractions containing the C-terminal portion of hCGβ were collected.

For removal of N-glycans, 0.5 U recombinant PNGase F (Roche) was added to 10 µg of hCG in 0.1 M sodium phosphate buffer pH 7.8. Deglycosylation was carried out for 48 h at 37 °C. Another 0.5 U of PNGase F was added after 24 h incubation. The removal of N-glycans was confirmed by SDS-PAGE in 12% w/v gel (Laemmli, U.K. 1970).

Mass spectrometry

For LC-MS analysis, the peptides were separated by RP-HPLC on a CapLC instrument (Waters) with a 0.075 x 150 mm C18 column (Atlantis dC18, 100 Å, 3 μm, Waters), which was eluted with a linear gradient of acetonitrile (5-50% in 30 min) in 0.1% formic acid. The flow rate was 0.3 μL/min and the eluent was directly injected into a quadrupole/time-of-flight hybrid mass spectrometer (Q-TOF Micro, Waters) equipped with an ESI source. The mass spectrometer was calibrated using 2 pmol/μL glufibrinogenic peptide B fragments as a standard.

Tandem mass spectrometric (MSMS) fragmentation spectra of the peptides were acquired by colliding the doubly or triply charged precursor ions with argon collision gas at accelerating voltages of 30-45 V.

For ESI-MS analysis of the chromatographically purified C-terminal fragment of hCGβ, the polypeptide was injected into the mass spectrometer (Q-TOF Micro, Waters) via a nanoflow interface with a Hamilton-syringe pump with a flow-rate of 0.3 μL/min. The mass spectrometer was calibrated using 400 fmol/μL myoglobin (Sigma) as a standard.

Differential data analysis

Mass spectra collected during the LC-MS separation of hCGβ peptides were exported into ASCII text files using the DataBridge of the MassLynx software (Waters). The text files were imported into DeCyder MS software (GE Healthcare), where different elution profiles were visualized as two-dimensional (2D) maps with m/z on y-axis and retention time on x-axis as well as three-dimensional (3D) graphs with intensity based on ion count as z-axis. Peptide eluting at specific time point and represented by number of different charge states was detected automatically, its charge states were

assigned, MS signal ion counts of different charge states were integrated and the actual mass of the peptide was deconvoluted. The ion counts of all different charge states of the same peptide were taken into account to calculate total intensity of deconvoluted mass in the range of 500-6000 Da. PepMatch module of DeCyder MS software was used to align peptides from different LC-MS runs and for semi quantitative differential analysis of the peptides. Ion counts over the spot areas manually selected were integrated and comparison of the integrated ion counts between samples was performed.

Acknowledgments

We would like to thank Ms Anne Ahmanheimo, Ms Taina Grönholm, Ms Maarit Leinimaa, Ms Jenni Sievänen and Ms Helena Taskinen for skillful technical assistance and Ms Ansa Karlberg for secretarial help. The financial support of the Finnish Academy of Sciences and European Union (LSHC-CT-2004-503011) is gratefully acknowledged.

Abbreviations

ESI, electrospray ionization

Fuc, fucose

Gal, galactose

GalNAc, N-acetylgalactosamine

GlcNAc, N-acetylglucosamine

hCG, human chorionic gonadotropin

hCGh, hyperglycosylated hCG

hCGn, nicked hCG

Hex, hexose

HexNAc, N-acetylhexosamine

LC, liquid chromatography

MAb, monoclonal antibody

Man, mannose

MS, mass spectrometry

MSMS, tandem mass spectrometry

NeuAc, N-acetylneuraminic acid

PNGase F, peptide-N-glycosidase F

RP, reverse-phase

Q-TOF, quadrupole/time-of-flight hybrid mass spectrometer

TFA, trifluoroacetic acid

References

Alfthan, H., Haglund, C., et al. (1992) Concentrations of human choriogonadotropin, its beta-subunit, and the core fragment of the beta-subunit in serum and urine of men and nonpregnant women. *Clin Chem*, **38**, 1981-1987.

Alfthan, H., Haglund, C., et al. (1992) Elevation of free beta subunit of human choriogonadotropin and core beta fragment of human choriogonadotropin in the serum and urine of patients with malignant pancreatic and biliary disease. *Cancer Res*, **52**, 4628-4633.

Aoyagi, Y., Isemura, M., et al. (1985) Fucosylated alpha-fetoprotein as marker of early hepatocellular carcinoma. *Lancet*, **2**, 1353-1354.

Benedet, J. and Pecorell, S. (2000) *Staging classifications and clinical practice guidelines of gynaecologic cancers*. FIGO Committe on Gynecologic Oncology. Elsevier.

Birken, S., Krichevsky, A., et al. (1999) Development and characterization of antibodies to a nicked and hyperglycosylated form of hCG from a choriocarcinoma patient: generation of antibodies that differentiate between pregnancy hCG and choriocarcinoma hCG. *Endocrine*, **10**, 137-144.

Birken, S., Yershova, O., et al. (2003) Analysis of human choriogonadotropin core 2 o-glycan isoforms. *Mol Cell Endocrinol*, **204**, 21-30.

Carlsen, R.B., Bahl, O.P., et al. (1973) Human chorionic gonadotropin. Linear amino acid sequence of the beta subunit. *J Biol Chem*, **248**, 6810-6827.

Cole, L.A., Kardana, A., et al. (1991) The heterogeneity of human chorionic gonadotropin (hCG). III. The occurrence and biological and immunological activities of nicked hCG. *Endocrinology*, **129**, 1559-1567.

Cole, L.A., Shahabi, S., et al. (1999) Hyperglycosylated human chorionic gonadotropin (invasive trophoblast antigen) immunoassay: A new basis for gestational Down syndrome screening. *Clin Chem*, **45**, 2109-2119.

Elliott, M.M., Kardana, A., et al. (1997) Carbohydrate and peptide structure of the alpha- and beta-subunits of human chorionic gonadotropin from normal and aberrant pregnancy and choriocarcinoma. *Endocrine*, **7**, 15-32.

Gervais, A., Hammel, Y.A., et al. (2003) Glycosylation of human recombinant gonadotrophins: characterization and batch-to-batch consistency. *Glycobiology*, **13**, 179-189.

Hakomori, S. (2002) Glycosylation defining cancer malignancy: new wine in an old bottle. *Proc Natl Acad Sci U S A*, **99**, 10231-10233.

Harvey, D.J. (2001) Ionization and collision-induced fragmentation of N-linked and related carbohydrates using divalent cations. *J Am Soc Mass Spectrom*, **12**, 926-937.

Jacoby, E.S., Kicman, A.T., et al. (2000) Determination of the glycoforms of human chorionic gonadotropin beta-core fragment by matrix-assisted laser desorption/ionization time-of-flight mass spectrometry. *Clin Chem*, **46**, 1796-1803.

Kelly, L.S., Kozak, M., et al. (2005) Lectin immunoassays using antibody fragments to detect glycoforms of human chorionic gonadotropin secreted by choriocarcinoma cells. *Anal Biochem*, **338**, 253-262.

Kessler, M.J., Mise, T., et al. (1979) Structure and location of the O-glycosidic carbohydrate units of human chorionic gonadotropin. *J Biol Chem*, **254**, 7909-7914.

Kessler, M.J., Reddy, M.S., et al. (1979) Structures of N-glycosidic carbohydrate units of human chorionic gonadotropin. *J Biol Chem*, **254**, 7901-7908.

Kobata, A. and Takeuchi, M. (1999) Structure, pathology and function of the N-linked sugar chains of human chorionic gonadotropin. *Biochim Biophys Acta*, **1455**, 315-326.

Kovalevskaya, G., Birken, S., et al. (2002) Differential expression of human chorionic gonadotropin (hCG) glycosylation isoforms in failing and continuing pregnancies: preliminary characterization of the hyperglycosylated hCG epitope. *J Endocrinol*, **172**, 497-506.

Laemmli, U.K. (1970) Cleavage of structural proteins during the assembly of the head of bacteriophage T4. *Nature*, **227**, 680-685.

Laidler, P., Cowan, D.A., et al. (1995) Tryptic mapping of human chorionic gonadotropin by matrix-assisted laser desorption/ionization mass spectrometry. *Rapid Commun Mass Spectrom*, **9**, 1021-1026.

Liu, C. and Bowers, L.D. (1997) Mass spectrometric characterization of the beta-subunit of human chorionic gonadotropin. *J Mass Spectrom*, **32**, 33-42.

Lustbader, J.W., Lobel, L., et al. (1998) Structural and molecular studies of human chorionic gonadotropin and its receptor. *Recent Prog Horm Res*, **53**, 395-424; discussion 424-395.

Mizuochi, T., Nishimura, R., et al. (1983) Structures of the asparagine-linked sugar chains of human chorionic gonadotropin produced in choriocarcinoma. Appearance of triantennary sugar chains and unique biantennary sugar chains. *J Biol Chem*, **258**, 14126-14129.

Pettersson, K., Siitari, H., et al. (1983) Time-resolved fluoroimmunoassay of human choriogonadotropin. *Clin Chem*, **29**, 60-64.

Puisieux, A., Bellet, D., et al. (1990) Occurrence of fragmentation of free and combined forms of the beta-subunit of human chorionic gonadotropin. *Endocrinology*, **126**, 687-694.

Skold, K., Svensson, M., et al. (2002) A neuroproteomic approach to targeting neuropeptides in the brain. *Proteomics*, **2**, 447-454.

Sobin, L. and Wittekind, C. (2002) *TNM classification of malignant tumours*. International Union Against Cancer (UICC). Wiley-Liss, New York.

Stenman, U.H., Alfthan, H., et al. (2004) Human chorionic gonadotropin in cancer. *Clin Biochem*, **37**, 549-561.

Weisshaar, G., Hiyama, J., et al. (1991) Site-specific N-glycosylation of human chorionic gonadotrophin--structural analysis of glycopeptides by one- and two-dimensional 1H NMR spectroscopy. *Glycobiology*, **1**, 393-404.

Legends to figures

Figure 1. Visualization of tryptic peptides of hCGβ by LC-MS. Panel A shows LC-MS separation of tryptic peptides of hCGβ purified from the urine of a testicular cancer patient before and after the PNGase F treatment (panel B). Panel C visualizes in a 3D mode the tryptic peptide P12 (m/z 637.3, $[M+2H]^{2+}$, Mw 1272.5) representing peptides existing in equal amounts in the two digests. A putatively N-glycosylated peptide (m/z 943.4, $[M+4H]^{4+}$, Mw 3769.6) absent from the PNGase F treated digest is visualized in panel D. Panel E shows the MS/MS fragmentation spectra of $[M+3H]^{3+}$ precursor ion m/z 1257.5 (Mw 3769.6) and the sugar-specific oxonium ions as well as oligosaccharide fragmentation patterns. Symbols: ■ HexNAc, ● Hex, ▲ Fuc, ◊ NeuAc

Figure 2. Structures and relative intensities of the glycans attached to Asn-13 of hCGβ. Panel A shows P3 containing various oligosaccharides from the urine of a normally pregnant woman at 35 weeks of pregnancy, panel B from the urine of a patient suffering from invasive mole and panel C from the urine of a patient with testicular cancer. The proposed sugar structures have been calculated by the mass matching approach, where the theoretical polypeptide mass of P3 is subtracted from the observed masses. Triantennary glycan structures are shown in black, biantennary in gray, monoantennary in white and the peptide without glycan is shown with lines. Symbols: ■ GlcNAc, ○ Man, ● Gal, ▲ Fuc, ◊ NeuAc. Fuc is attached to the first GlcNAc within the structures when present.

Figure 3. Structures and relative intensities of the glycans attached to Asn-30 of hCGβ. P4 containing oligosaccharides purified from the urine of a pregnant woman are shown in panel A, from the urine of an invasive mole patient in panel B and from the urine of a testicular cancer patient in panel C. The proposed sugar structures are calculated by the mass matching approach. Triantennary glycan structures are shown in black, biantennary in grey and monoantennary in white. Symbols are as in Figure 2.

Figure 4. ESI-MS analysis of the C-terminal part of hCGβ. The deconvoluted spectra of GluC-cleaved hCGβ C-terminal fragment from the urine of a pregnant woman (panel A), an invasive mole patient (panel B) and a testicular cancer patient (panel C) are shown. Panel D indicates the theoretical masses of different monosaccharide compositions when attached to the C-terminal polypeptide and visualizes their matches to the observed masses. The most intense mass observed in different samples is shown in bold typeface.

Figure 5. Structures and relative intensities of the glycans attached to Ser-121, Ser-127, Ser-132 and Ser-138 of the hCGβ. P13 containing oligosaccharides are shown in Panel A, P15 containing oligosaccharides in Panel B and P14 containing structures in Panel C. The glycans of hCGβ purified from the urine of a pregnant woman are visualized in white, from the urine of an invasive mole patient in grey and from the urine of a testicular cancer patient in black. The proposed sugar structures attached to Ser-121 (A) and Ser-138 (B) are calculated by the mass matching approach. In panel C putative structures attached to P14 are clustered into four categories to represent different sugar structures capable of occurring in Ser-127 and Ser-132: 1) one core-1, 2) two core-1 or one core-2, 3) one core-2 and one core-1 or 4) two core-2 glycans.

Proposed structures are gathered under the vertical lines pointing the masses capable of representing the structures. Symbols: □ GalNAc, ■ GlcNAc, ● Gal, ◊ NeuAc

Table I. Amino acid sequence of hCGβ and peptides derived by trypsin digestion. The theoretical trypsin cleavage sites are indicated by vertical lines, the four glycosylated amino acids, Asn-13, Asn-30, Ser-121, Ser-127, Ser-132, Ser-138, are highlighted in bold. The most C-terminal GluC cleavage site is indicated by a dashed vertical line (panel A). Observed m/z values, charge states and deduced masses of tryptic peptides derived from 4-vinylpyridine-alkylated hCGβ purified from the urine of a testicular cancer patient are shown in panel B. Peptide sequences assigned for each observed mass is indicated by amino acid positions and the theoretical mass of the assigned sequence is shown.

A

1	S	K	E	P	L	R	P	R	C	R	P	I	**N**	A	T	L	A	V	E	K	E	G	C	23
24	P	V	C	I	T	V	**N**	T	T	I	C	A	G	Y	C	P	T	M	T	R	V	L	Q	46
47	G	V	L	P	A	L	P	Q	V	V	C	N	Y	R	D	V	R	F	E	S	I	R	L	69
70	P	G	C	P	R	G	V	N	P	V	V	S	Y	A	V	A	L	S	C	Q	C	A	L	92
93	C	R	R	S	T	T	D	C	G	G	P	K	D	H	P	L	T	C	D	D	P	R	F	115
116	Q	D	S	S	S	**S**	K	A	P	P	P	**S**	L	P	S	P	**S**	R	L	P	G	P	**S**	138
139	D	T	P	I	L	P	Q																	145

B

Peptide	Position (amino acids)	Observed m/z[d]	Charge state	Deduced m (Da)	Theoretical m (Da)
P1+P2	1-8	491.787	2	981.558	981.572
P3[a,c]	9-20				1418.770
P4[a,c]	21-43				2852.298
P5[c]	44-60	658.692	3	1973.052	1973.092
P5+P6[c]	44-63	782.091	3	2343.249	2343.288
P7	64-68	651.342	1	650.334	650.339
P8[c]	69-74	747.392	1	746.384	746.390
P9[c]	75-94	592.796	4	2367.152	2367.169
P9+P10[c]	75-95	631.817	4	2523.236	2523.270
P11+P12[c]	96-114	742.321	3	2223.939	2223.968
P12[c]	105-114	637.274	2	1272.532	1272.556
P13[b]	115-122				884.388
P14[b]	123-133				1104.593
P15[b]	134-145				1233.660

[a] N-glycosylation site
[b] O-glycosylation site(s)
[c] ethylpyridyl-modified cysteines
[d] at highest intensity

Table II. Glycan composition of hCG isolated from urine of two testicular cancer patients with stage 1 (TCa1) and stage 3 disease (TCa3,), one choriocarcinoma patient (ChCa), one patient with an invasive mole (Mole) and from pregnant (P) women at different times of gestation. A commercially available preparation of urinary hCG (Pregn) and hCG isolated from the spent medium from a choriocarcinoma cell line (JEG) are also shown. The proportions of different oligosaccharide structures present on P3, P4, P13, P14 and P15 were calculated on the basis of the relative intensities of glycopeptides detected by LC-MS (A). The degree of fucosylation of the N-glycans in P3 and P4 is shown in panel B. P3 and P4 contain one N-glycan each, P13 and P15 one O-glycan each and P14 two O-glycans.

A

	TCa1	TCa3	ChCa	JEG	Mole	P 5wk	P 7wk	P 35wk	P 35wk	Pregn
P3 (Asn-13)										
without glycan	7.7	2.5	1.4	3.9	5.1	1.9	4.1	5.5	4.3	2.7
+ monoantennary	32.5	32.6	20.0	33.3	26.9	30.1	21.7	22.6	11.9	18.3
+ biantennary	36.1	44.2	61.5	52.1	40.7	47.2	59.9	44.6	57.2	65.7
+ triantennary	20.0	17.5	15.9	10.7	24.0	18.3	14.0	26.4	25.6	12.7
+ tetra-antennary	3.6	3.1	1.2	0	3.4	2.5	0.2	1.0	0.9	0.6
P4 (Asn-30)										
without glycan	1.0	0.4	0	0	1.1	0.4	0.2	0.6	0.5	0.8
+ monoantennary	33.5	23.9	4.4	4.1	18.9	15.3	15.9	18.2	11.8	12.0
+ biantennary	33.7	36.9	81.8	90.7	60.6	67.0	78.4	72.2	76.5	83.9
+ triantennary	29.7	38.1	13.2	5.2	19.4	17.3	5.5	9.0	11.1	3.2
+ tetra-antennary	2.0	0.7	0.6	0	0	0	0	0	0.1	0
P13 (Ser-121)										
without glycan	2.7	2.9	2.1	0.8	7.2	1.7	2.4	8.0	1.3	3.1
+ core-1	12.9	13.2	11.5	3.6	24.1	9.1	12.7	23.7	14.2	29.3
+ core-2	84.4	83.9	86.4	95.6	68.7	89.2	84.9	68.3	84.5	67.7
P14 (Ser-127,Ser-132)										
without glycan	0	0	0	0	0	1.0	2.5	6.4	2.5	0.7
+ 1 core-1	0.8	1.9	2.5	1.9	40.0	36.0	68.1	91.6	62.1	24.5
+ 2 core-1 or 1 core-2	13.2	29.7	66.5	40.4	53.5	26.2	18.5	2.0	32.5	52.4
+ 1 core-2 and 1 core-1	49.8	55.9	29.3	48.9	6.5	30.2	10.8	0	2.9	20.7
+ 2 core-2	36.1	12.5	1.7	8.8	0	6.6	0	0	0	1.7
P15 (Ser-138)										
without glycan	8.0	21.1	30.9	10.4	15.4	13.3	14.2	25.0	14.2	9.1
+ core-1	55.1	67.2	64.8	69.0	84.6	70.7	81.6	69.6	84.9	82.0
+ core-2	36.8	11.7	4.3	20.7	0	16.0	4.1	5.4	0.9	8.9

B

	TCa1	TCa3	ChCa	JEG	Mole	P 5wk	P 7wk	P 35wk	P 35wk	Pregn
P3 glycans										
- fucose	63.6	53.2	58.2	86.8	43.7	63.6	76.5	96.4	76.5	73.9
+ fucose	36.4	46.8	41.8	13.2	56.3	36.4	23.5	3.6	23.5	26.1
P4 glycans										
- fucose	15.2	4.3	1.5	18.3	0	4.1	12.0	21.4	5.8	13.2
+ fucose	84.8	95.7	98.5	81.7	100.0	95.9	88.0	78.6	94.2	86.8

Table III. Glycan composition of various forms of hCGβ isolated from urine of a patient with hydatidiform mole. Panel A shows the percentages of the main structures present and panel B the degree of fucosylation on the N-glycans. Intact heterodimeric hCG (U-hCG), free β-subunit (U-hCGβ) and "hyperglycosylated" hCG (U-hCGh) were purified from urine and heterodimeric hCG also from serum (S-hCG). P3 and P4 contain one N-glycan each, P13 and P15 one O-glycan each and P14 two O-glycans.

A

	U-hCG	U-hCGβ	U-hCGh	S-hCG
P3 (Asn-13)				
without glycan	5.1	0.5	3.4	2.2
+ monoantennary	26.9	7.9	26.1	20.8
+ biantennary	40.7	45.4	46.3	53.9
+ triantennary	24.0	37.2	21.8	19.8
+ tetra-antennary	3.4	8.9	2.3	3.3
P4 (Asn-30)				
without glycan	1.1	0	0.7	0.3
+ monoantennary	18.9	4.2	15.4	13.6
+ biantennary	60.6	61.4	55.6	65.3
+ triantennary	19.4	30.0	28.3	19.8
+ tetra-antennary	0.0	4.4	0	1.0
P13 (Ser-121)				
without glycan	7.2	2.2	1.0	2.1
+ core-1	24.1	12.9	3.4	16.5
+ core-2	68.7	85.0	95.6	81.4
P14 (Ser-127,Ser-132)				
without glycan	0	0	0	3.5
+ 1 core-1	40.0	13.8	1.0	63.7
+ 2 core-1 or 1 core-2	53.5	36.5	20.3	20.3
+ 1 core-2 and 1 core-1	6.5	49.7	73.9	11.1
+ 2 core-2	0	0	4.8	1.4
P15 (Ser-138)				
without glycan	15.4	15.4	26.9	21.8
+ core-1	84.6	78.7	73.1	74.9
+ core-2	0	5.9	0	3.3

B

	U-hCG	U-hCGβ	U-hCGh	S-hCG
P3 glycans				
- fucose	43.7	16.4	41.0	50.0
+ fucose	56.3	83.6	59.0	50.0
P4 glycans				
- fucose	0	0	2.5	3.9
+ fucose	100.0	100.0	97.5	96.1

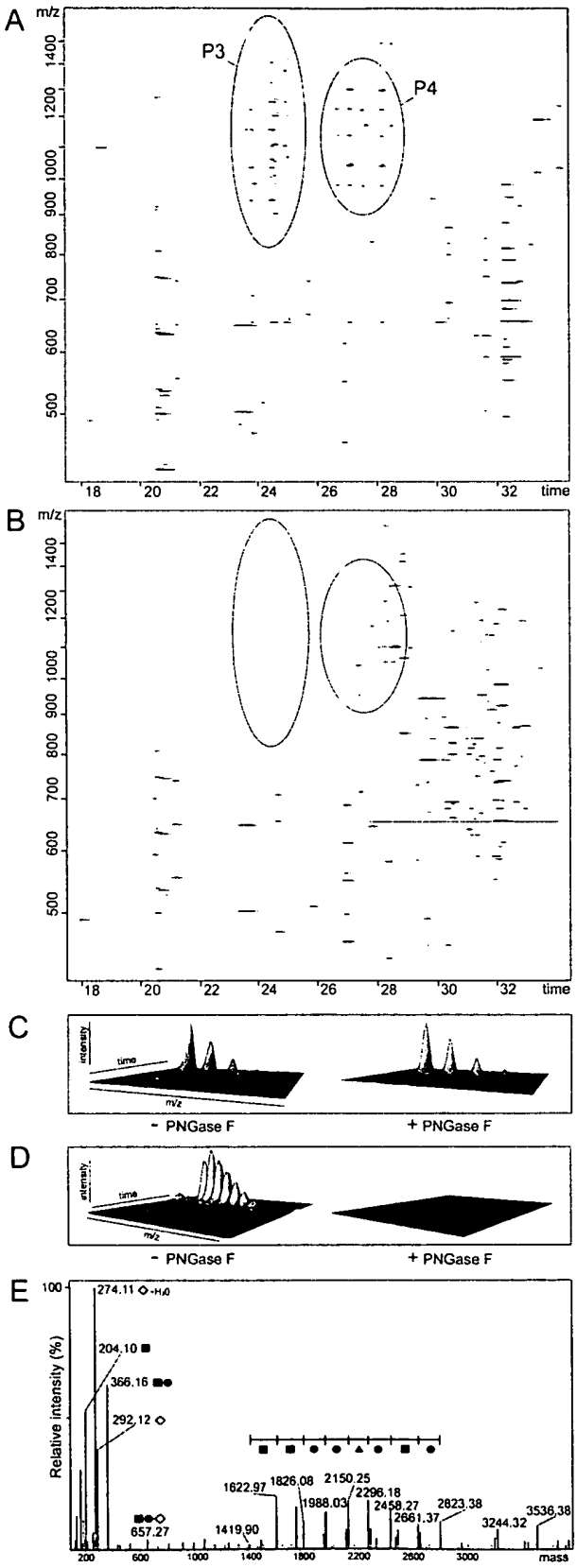

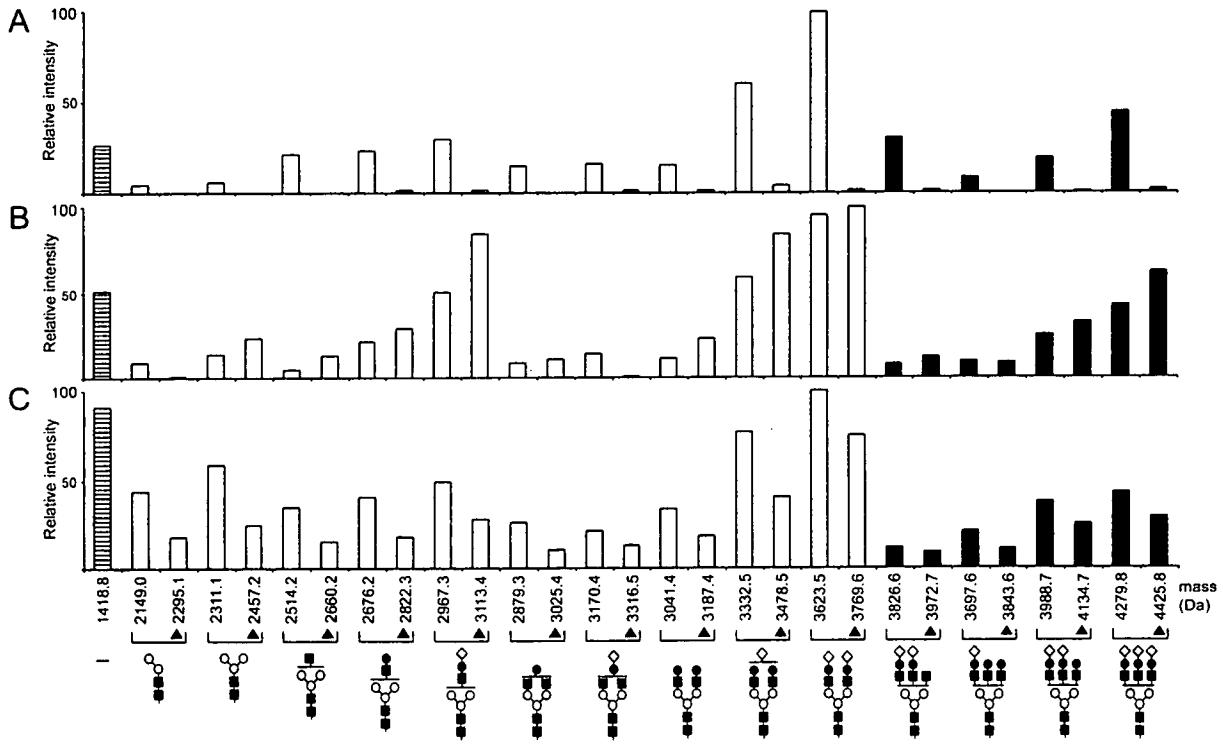
A
B
C
100
50
Relative intensity
1418.8
2149.0
2295.1
2311.1
2457.2
2514.2
2660.2
2676.2
2822.3
2967.3
3113.4
2879.3
3025.4
3170.4
3316.5
3041.4
3187.4
3332.5
3478.5
3623.5
3769.6
3826.6
3972.7
3697.6
3843.6
3988.7
4134.7
4279.8
4425.8
mass
(Da)

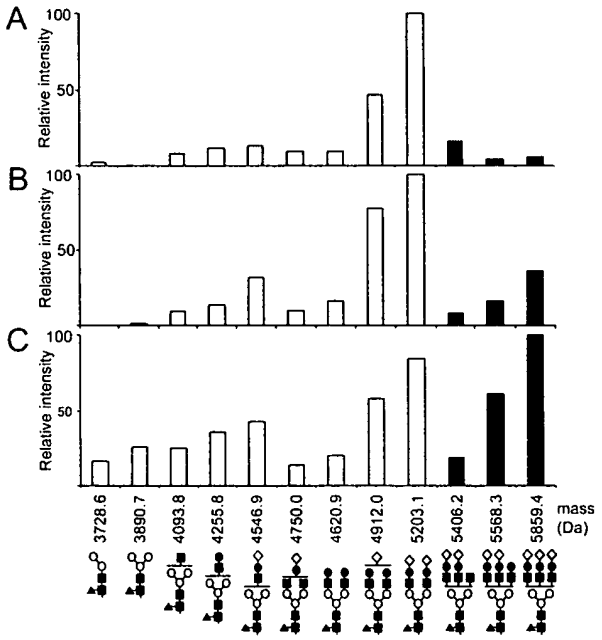
A
B
C
100
50
Relative intensity
3728.6
3890.7
4093.8
4255.8
4546.9
4750.0
4620.9
4912.0
5203.1
5406.2
5568.3
5859.4
mass
(Da)

A

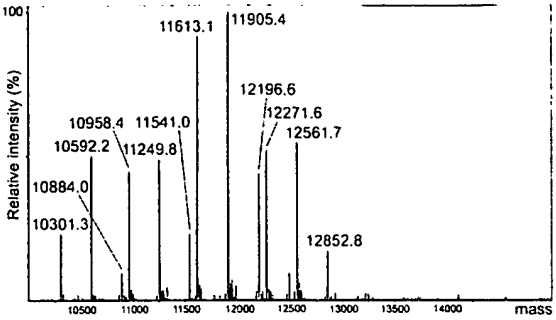

B

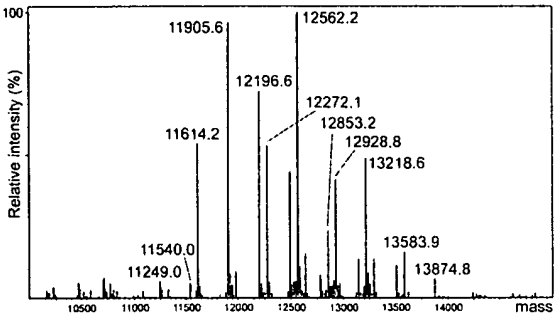

C

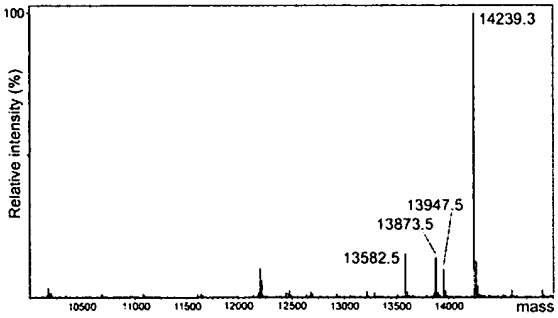

D

	Theoretical m (Da)	Observed		
		Preg 35w	Mole	TestisCA
hCGβ C-terminus (aa 66-145)[a]	8988.3			
+ $HexNAc_2Hex_2NeuAc_2$	10300.8	x		
+ $HexNAc_2Hex_2NeuAc_3$	10591.9	x		
+ $HexNAc_2Hex_2NeuAc_4$	10883.0	x		
+ $HexNAc_3Hex_3NeuAc_3$	10957.0	x		
+ $HexNAc_3Hex_3NeuAc_4$	11248.1	x	x	
+ $HexNAc_3Hex_3NeuAc_5$	11539.2	x	x	
+ $HexNAc_4Hex_4NeuAc_4$	11612.5	x	x	
+ $HexNAc_4Hex_4NeuAc_5$	11903.8	x	x	
+ $HexNAc_4Hex_4NeuAc_6$	12195.1	x	x	
+ $HexNAc_5Hex_5NeuAc_5$	12271.3	x	x	
+ $HexNAc_5Hex_5NeuAc_6$	12560.4	x	x	
+ $HexNAc_5Hex_5NeuAc_7$	12851.7	x	x	
+ $HexNAc_6Hex_6NeuAc_6$	12927.9		x	
+ $HexNAc_6Hex_6NeuAc_7$	13216.8		x	
+ $HexNAc_7Hex_7NeuAc_7$	13581.9		x	x
+ $HexNAc_7Hex_7NeuAc_8$	13873.0		x	x
+ $HexNAc_8Hex_8NeuAc_7$	13946.9			x
+ $HexNAc_8Hex_8NeuAc_8$	14238.2			x

[a] ethylpyridyl-modified cysteines

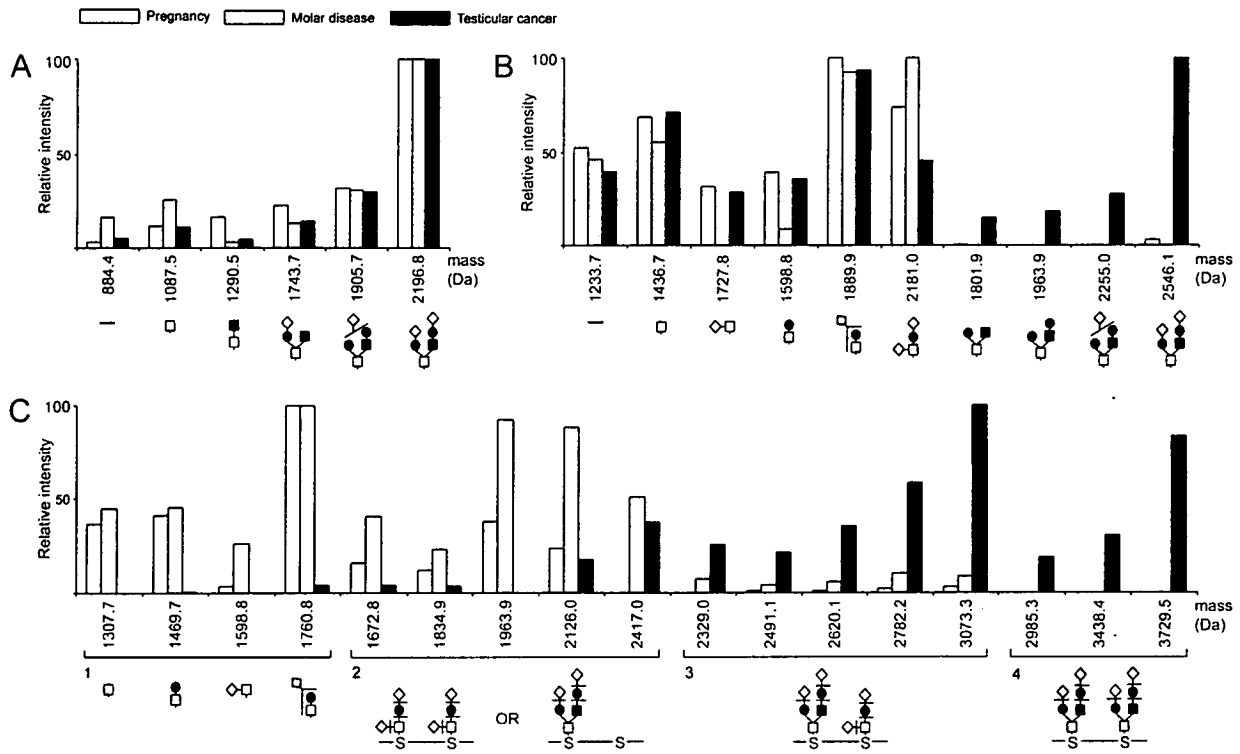
Pregnancy
Molar disease
Testicular cancer
A
B
C
Relative intensity
100
50
mass (Da)
884.4
1087.5
1290.5
1743.7
1905.7
2196.8
1233.7
1436.7
1727.8
1598.8
1889.9
2181.0
1801.9
1963.9
2255.0
2546.1
1307.7
1469.7
1598.8
1760.8
1672.8
1834.9
1963.9
2126.0
2417.0
2329.0
2491.1
2620.1
2782.2
3073.3
2985.3
3438.4
3729.5
1
2
3
4
OR
S
S